International Journal of Current Research and Modern Education (IJCRME)
ISSN (Online): 2455 – 5428 & Impact Factor: 3.165
Special Issue, NCFTCCPS - 2016

A NOVEL FLYBACK INVERTER WITH REDUCED SWITCHES

R. Meiyazhagan* & S. Usha**
S.R.G Engineering College, Namakkal, Tamilnadu

Abstract:

This paper presents analysis, design, and implementation of an isolated grid-connected inverter for photovoltaic (PV) applications based on interleaved flyback converter topology operating in discontinuous current mode. In today's PV inverter technology, the simple and the low-cost advantage of the flyback topology is promoted only at very low power as microinverter. Therefore, the primary objective of this study is to design the flyback converter at high power and demonstrate its practicality with good performance as a central-type PV inverter. For this purpose, an inverter system rated at 2 kW is developed by interleaving of only three flyback cells with added benefit of reduced size of passive filtering elements. A simulation model is developed in the piece-wise linear electrical circuit simulator. Then, the design is verified and optimized for the best performance based on the simulation results. Finally, a prototype at rated power is built and evaluated under the realistic conditions. The efficiency of the inverter, the total harmonic distortion of the grid current, and the power factor are measured as 90.16%, 4.42%, and 0.998, respectively. Consequently, it is demonstrated that the performance of the proposed system is comparable to the commercial isolated PV inverters in the market, but it may have some cost advantage.

1. Introduction:

Table and freely available source of energy and the candidate to play a greater role in the energy market of the world in the near future [1]. Therefore, the research and development in the solar technology field is in the rise [2]–[6], [8]–[20], [22], [25]. However, the high cost of the technology still limits its usage globally. The low cost is greatly important for commercialization especially in small electric power systems including the residential applications [2]–[6]. Therefore, the primary objective of the study presented in this paper is to contribute to the research and development in the photovoltaic (PV) inverter technology by trying the flyback topology at high power. If it is implemented effectively with good performance, the developed inverter system can be a low-cost alternative to the commercial isolated grid-connected PV inverters in the market.

The simple structure of the flyback topology and easy power flow control with high power quality at the grid interface are the key motivations for this work. The flyback converter is recognized as the lowest cost converter among the isolated topologies since it uses the least number of components. This advantage comes from the ability of the flyback topology combining the energy storage inductor with the transformer. In other type of isolated topologies, the energy storage inductor and the trans-former are separate elements. While the inductor is responsible for energy storage, the transformer on the other hand is responsible for energy transfer over a galvanic isolation [7]. The combination of these two components in a flyback topology eliminates the bulky and costly energy storage inductor and therefore leads to a reduction in cost and size of the converter. However, we have to make it clear here that the cost depends on the implementation as much as the selected topology, so not every implementation of the flyback topology leads to a low-cost converter. For this reason, as we try to achieve the high-power implementation of the flyback converter with good

performance, which is our primary research contribution, we will also try to preserve the cost advantage during the final implementation step.

Practical implementation of a transformer with relatively large energy storage capability is always a challenge. The air gap is where the energy is stored, so a high-power flyback converter design needs a relatively large air gap. As a result of this, the magnetizing inductance is going to be quite small. The aforementioned challenge is actually achieving such a small magnetizing inductance with low leakage inductance. A fly-back converter built with a transformer that has large leakage flux and poor coupling will have poor energy transfer efficiency. Mainly for this reason, the flyback converters are generally not designed for high power. As a result, the flyback topology finds a limited role in PV applications only at very low power as micro inverter [10]–[13]. In this technology, every PV panel comes with a dedicated energy conversion unit; a micro inverter attached to the output terminals. For this reason, the technology is also named as ac PV module application [14]–[18]. In this practice, many such ac PV modules are connected in parallel to get the desired power output. The maximum harvesting of solar energy in this method is the best since there is a dedicated maximum power point tracker (MPPT) for each PV panel [19]. However, the overall cost of this application is higher compared to the central-type inverter systems.

Nevertheless, when advanced design methods are employed effectively, single-stage flyback converters can be designed and used in high power applications as well. Furthermore, the interleaving of these high power flyback stages (cells) facilitates developing a central-type PV inverter. The added bene-fit of interleaving is that the frequency of the ripple components (undesired harmonics) at the waveforms are increased in proportion to the number of interleaved cells. This feature fa-cilitates easy filtering of the ripple components or using smaller sized filtering elements. The ability to reduce the size of pas-sive elements is beneficial for reducing the cost and obtaining a compact converter [21]. Fig. 1 shows the block diagram of the proposed inverter system. The results of an earlier work based on the same topology where the primary objective was to prove the concept with a design at 1 kW were presented in [26]. Since the time of that work, there have been major design changes and upgrades in order to process twice more power and at the same to achieve better overall performance.

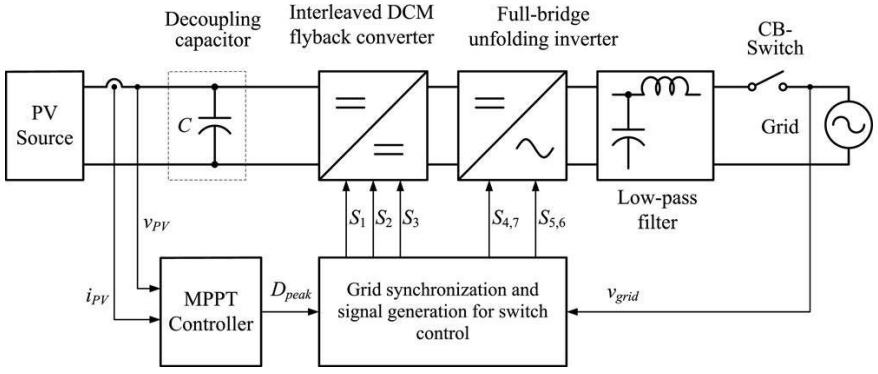

Figure 1: Block diagram of the proposed grid connected PV inverter system based on interleaved DCM flyback converter topology.

As mentioned before, the choice of operation mode for the converter is discontinuous current mode (DCM). The fundamental motivations for selecting DCM operation are summarized as follows.

1. It provides very fast dynamic response and a guaranteed stability for all operating conditions under consideration.

2. No reverse recovery problem. The diodes exhibits re-verse recovery problems in CCM operation which cause noise, electromagnetic interference problems, and additional losses. So, DCM operation eliminates all these complications.
3. No turn on losses.
4. Small size of the transformer.
5. Easy control. No need for a feedback loop for the control of the grid current. Only an open-loop control is enough to synthesize a sinusoidal current with good total harmonic distortion (THD). This makes the implementation of the control system less complex for DSP and allows faster execution time.

Contrary to the aforementioned great benefits of the DCM operation, it has several disadvantages as well. In this mode of operation, the current waveforms have higher form factor (high RMS to mean ratio) compared to continuous current mode (CCM). This normally leads to more power losses. So, as a solution, every current carrying path including the switching devices should have low resistivity. Another drawback of DCM operation is the current pulses with large peaks and high amount of discontinuity in the waveforms. Device paralleling is a way to handle the high peak currents. Nevertheless, these disadvantages can be considerably reduced by interleaving of several cells. As a first benefit, the current in each cell will have much less peak but the same amount of discontinuity. However, the discontinuity will be significantly reduced as soon as the cells connect at the common point. All this benefits come from the ability of phase-shifted several cells spreading the power flow evenly over the switching cycle with minimum discontinuity at the source and grid side. In brief, the effective interleaving has the potential to solve or greatly reduce the adverse effects of the DCM operation [21]. Consequently, the circuit diagram of the proposed inverter system based on three-cell interleaved DCM flyback converter topology is shown in Fig. 2.

In conclusion, this study has developed and presented the technology in full detail to produce a grid-tied, isolated, and central-type inverter based on the flyback converter topology at 2 kW, which is not available in today's PV market. The developed system has performed satisfactorily according to major specifications such as the efficiency and the THD of the grid current. Moreover, the study has developed high-power flyback transformers at 700 W and below with extremely low leak-age inductance. We also consider this outcome as the significant research contribution since this technology may lead to the development of different applications where the low cost and simplicity are always an issue.

The remainder of this paper is organized as follows. Section II describes the converter topology and defines the operating principles. Section III performs the analysis of the converter and derives the design equations. Section IV presents the design of the converter in steps. Sections V and VI give the simulation and the experimental results, respectively. Finally, Section VII provides the conclusions.

2. Converter Description and Operating Principles:

As shown in Fig. 2, the PV source is applied to a three-cell interleaved flyback converter through a decoupling capacitor. Each flyback converter uses a metal oxide semiconductor field-effect transistor (MOSFET) for switching at the primary side, a flyback transformer, and a diode at the secondary side. The topology also has to employ a full-bridge inverter and a low-pass filter for proper interface to the grid. When the flyback switches (S_1, S_2, S_3) are turned ON, a current flows from the common point (the PV source) into the magnetizing inductance of the flyback transformers, and energy is stored in the form of magnetic field. During the on time of the switches, no current flows

to the output due to the position of the secondary side diodes; therefore, energy to the grid is supplied by the capacitor C_f and the inductor L_f. When the flyback switches are turned OFF, the energy stored in the magnetizing inductances is transferred into the grid in the form of current. So, the flyback inverter acts like a voltage-controlled current source.

The converter is operated in DCM for easy and stable generation of ac currents at the grid interface. The DCM operation of converter under open-loop control produces triangular cur-rent pulses at every switching period. If sinusoidal pulse width modulation (PWM) method is used for control, the inverter will regulate these current pulses into a sinusoidal current in phase with the grid voltage [22]. Such currents are shown in Figs. 3 and 4 for a conceptual case. Specifically, Fig. 3 shows the conceptual flyback converter input currents and Fig. 4 shows

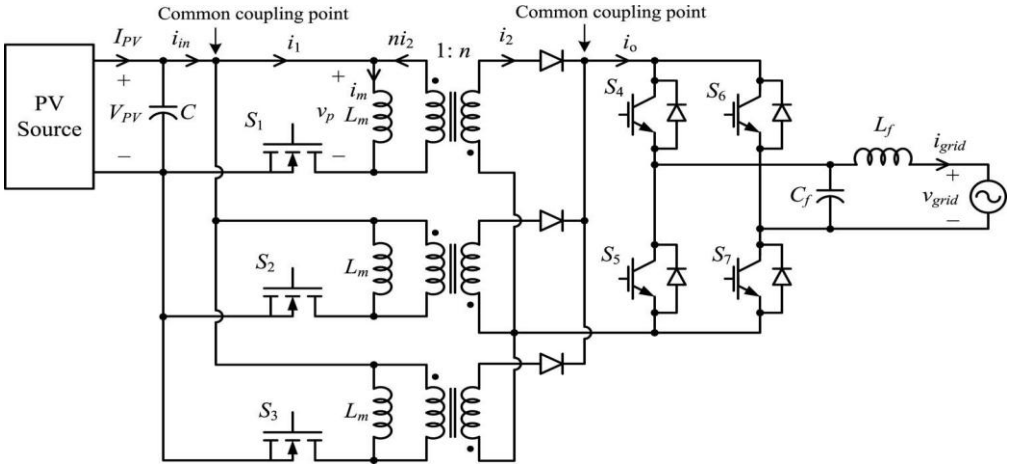

Figure 2: Circuit schematic of the proposed PV inverter system based on three cell interleaved flyback converter topology

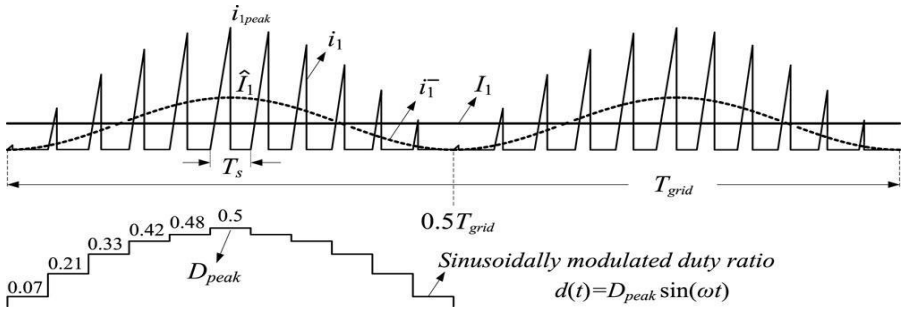

Figure 3: Instantaneous flyback converter input current (i_1), its instantaneous average ($\bar{i}_1$) over one switching period, and the extended average (I_1) over one I grid period, also the sinusoidally modulated duty ratio over one-half cycle of a grid period.

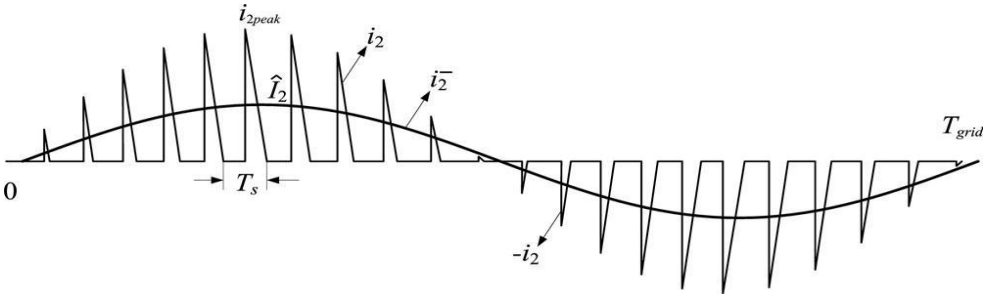

Figure 4: Instantaneous flyback converter output current (i_2) after unfolded by the full bridge inverter and its instantaneous average ($\bar{i}_2$) over one switching I period.

As it is seen, the instantaneous currents are composed of discontinuous current pulses with peaks that fall within a sinusoidal envelope since their pulse widths are sinusoid ally modulated. Figure 3 also shows the three components of the instantaneous flyback converter input current (i_1): the high frequency (switch-ing frequency) components, the low frequency (twice the line frequency) component (¯1) which is the instantaneous average I of i_1 over one switching period, and the dc component (I_1) which is the average over one grid period. In practice, a PV source is not an ideal voltage source; so any ac current that is supplied by it will cause variations at its terminal voltage.

So, for good performance of the converter as far as the power utilization and output current distortion, the voltage variations (ripple) across the PV module terminals should be as small as practically possible [20], [23]. For this reason, a decoupling capacitor is placed at the flyback converter input and sized in such a way that both the low and the high frequency ac components are bypassed sufficiently and only the dc (average) component I_1 is allowed to be supplied by the PV source. More explanations about this problem and sizing of decoupling capacitor are provided in the analysis section. Fig. 4 shows the instantaneous flyback converter output current (i_2) after unfolded by the full bridge inverter and its instantaneous average (¯2).

The full bridge inverter is only responsible for unfolding the sinusoid ally modulated dc current packs into ac at the right moment of the grid voltage. Since the switches of the inverter are operated at the grid frequency, the switching losses are insignificant. Only conduction losses are concerned. For this reason, the bridge can use thyristor or even transistor switches for lower cost. However, for easy control also the availability in the laboratory for fast prototyping, we prefer using insulated-gate bipolar transistor (IGBT) switches for this design. But, the final prototype will not use IGBTs. The low-pass filter after the IGBT inverter is responsible for supplying a current to the grid with low THD by removing the high frequency harmonics of the pulsed current waveforms.

3. Converter Analysis:

The analysis of the converter is performed based on the circuit schematic given in Fig. 2 and only considers the first flyback cell. And it is done over one particular switching period when both the grid voltage and the duty ratio are at their peak values. Later, the analysis results will be generalized to include all the cells and extended for the operation of the converter over a full grid period. Consequently, Fig. 5 shows the control signal for the flyback switch, flyback transformer primary voltage (v_p), and magnetization current (i_m) with its components i_1 and ni_2 over

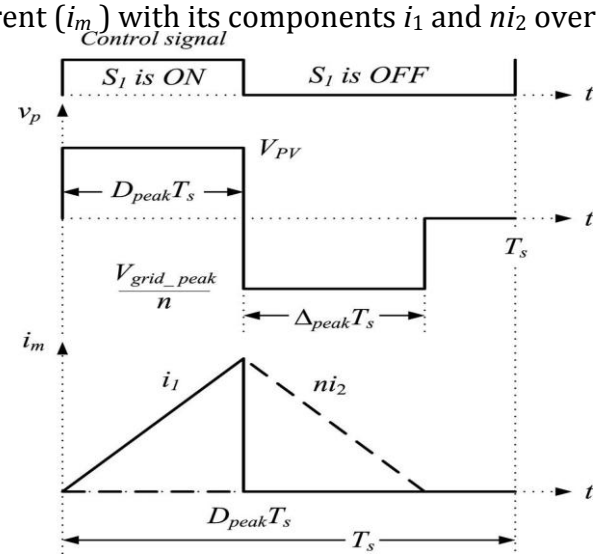

Figure 5: Flyback switch control signal, flyback transformer primary voltage (v_p), and magnetization current (i_m) with its components i_1 and ni_2 over the switching period when the grid voltage is at its peak. The selected switching period where the duty ratio is at its peak (D_{peak}). Note that the waveforms represent DCM operation.

A. Analysis When the Flyback Switch is Turned ON:

When S_1 is turned ON in Fig. 2, the PV voltage V_{PV} is applied to the primary winding and current flows in the primary circuit. The current starts from zero initial value and increases linearly with a positive slope assuming that V_{PV} is constant. The flyback input current (also the magnetizing current) in Fig. 5 can be defined as

Moreover, the half of this current gives the average (dc) cur-rent (I_1) that is drawn from the PV source.

Where I_{PV} is the current delivered by the PV source and n_{cell} is the number of the interleaved cells. Consequently, the relationship between the flyback converter parameters and the PV source output power can be written as follows:

At the design stage, the desired value of the magnetizing inductance of the flyback transformer (L_m) is computed using (5) based on the selected switching frequency, the optimum number of the interleaved cells, and the optimum D_{peak} value. The $D_{p\ eak}$ value is generated by the MPPT controller for maximum harvesting of the solar energy under different irradiation levels and applied to the flyback switches. Note that the entry for V_{PV} in (5) is the PV voltage at MPP.

B. Analysis When the Flyback Switch is Turned OFF:

When S_1 is turned OFF in Fig. 2, the flyback transformer primary voltage becomes negative of the grid voltage after scaled by the turn ratio as shown in Fig. 5. The magnetizing current for this case can be written as follows:

$$\overline{ni2} = im = {}^{Vgrid}\ t\ (6)\ nL_m$$

Where $\hat{}_{grid}$ is the peak of the grid voltage and is the flyback transformer turn ratio. At the end of the switch off time, the magnetizing current decreases from its maximum value to zero linearly. The change in the current is given as follows:

Where is the ratio of the time that takes for the magnetizing current to reset as shown in Fig. 5. It can be computed by equating the Volt–second area across the primary voltage (v_p) as follows:

Where f_s is the switching frequency. This particular maximum is the peak value of the largest of the sinusoid ally modulated triangular current pulses within a half-grid period shown in Fig. 3. The area of this triangle also gives the peak value of the twice the line frequency component of the flyback input current, which is given as follows: Knowing peak allows finding the peak value of the instantaneous average of the flyback output current ($\bar{}2$), which is the I area of the largest of the triangular current pulses within a grid period as shown in Fig. 4. Following gives this peak value: manufactured by different companies as long as the PV voltage and power range are matched. Hence, the PV source selected for the current design uses five BP365 PV panels in a string and six strings in parallel yielding a maximum power of 1950 W at the PV terminals as given in Table I. As mentioned earlier, the experimental setup will use different PV panels with similar characteristics or a PV simulator but provide the same rated output power.

B. Flyback Transformer Design:

The success of the proposed inverter system is very much related to the success in the design and the practical realization of the flyback transformers. As aforementioned, the flyback trans-formers have to store large amount of energy and then transfer it to the output through magnetic coupling at every switching cycle. Therefore, during the design process, the strategies that first create the most effective

energy storage mechanism and second the most optimum and efficient energy transfer path must be employed.

Firstly, the magnetizing inductance of the flyback transformer L_m is determined under nominal conditions. Using 88 V for V_{PV}, 40 kHz for f_s , 1950 W for P_{PV} , 3 for n_{cell} , and 0.3333 for $D_{p\ eak}$ in (5), L_m is calculated as 8.27 μH. Rounding this result to 8 μH and reworking (5), the practical value of $D_{p\ eak}$ is calculated as 0.3278. Then, the turn's ratio of the transformer is determined for the minimum the grid voltage. Using 202 V for $\hat{}_{grid}$ (minimum peak grid voltage), 88 V for PV, and 0.3278 for V V in (11), the turns ratio (n) is determined as 4.7. But, it is selected as 4.5 for practical implementation. For this design, we selected to use the bar-shaped I93/28/30 part numbered ferrite core with 840 mm^2 cross-sectional area made by Ferro cube based on 3C94 material. Using 840 mm^2 for A_{core} and 4 for N and 8 μH for L_m in (12), the air gap length is found as 2.11 mm.

The next major objective in the design of the flyback trans-former is to obtain the lowest leakage inductance. This must be achieved for efficient energy transfer to the output. In order to obtain practically the lowest leakage inductance, we have employed the following techniques that are also reported in the recent literature [21].

1) Making the coil and core heights longer so that flux lines can be stretched and forced more into the core, which improves coupling.
2) Reducing the number of winding layers so that less space between the layers. The leakage increases as the number of layers is increased. To reduce layer height, the practically lowest number turns should be used. The low-voltage winding uses four turns and the high-voltage winding uses 18 turns to get the turn's ratio of 4.5. The selected number of turns should enable sandwiching of the windings.
3) Using sandwiched windings so that the magnetic field inside the window area is reduced. One level of sandwiching of windings reduces the leakage inductance up to one-fourth compared to the no sandwiched case [21]. In this application, the low-voltage winding is divided into two halves. Then, the 18 turns of the high voltage winding is sandwiched between these two halves.

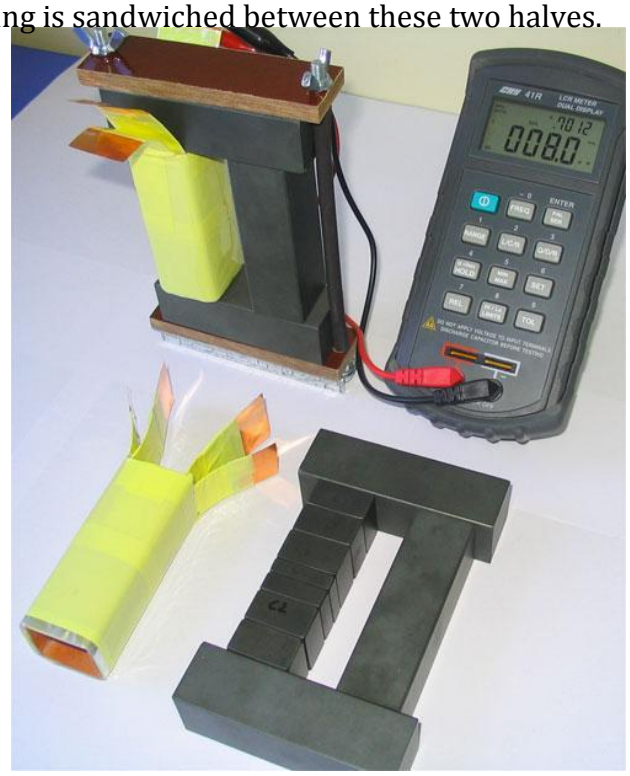

Figure 6: Flyback transformer constructed for the prototype converter.

4) The terminal leads are made using copper strips with wide surface area instead of round conductors. This method minimizes the parasitic inductance when the high-power flyback transformer is connected to the printed circuit boards. The parasitic inductance would be large if round conductors were used.
5) Distributing of the air gap along the core structure so that fringing flux is minimized. The distributed air gap also contributes to the low leakage by improving the coupling. The air gap length, which is 2.11 mm, is divided into six sections and distributed along one core leg each gap being 0.352 mm as shown in Fig. 6. The top and bottom hori-zontal bars directly press against the vertical bars without any air gap. So, the major air gap effect is localized in the sliced leg.

The flyback transformer designed and constructed according to previous considerations is shown in Fig. 6. The thickness of the copper foils used for making the windings is selected less than the skin depth requirement at 40 kHz. Also the cross-sectional area of the coppers is more than required. The peak flux density in the core is 0.215 T. The total copper and core losses averaged over a grid cycle are 21.88 W. The magnetizing inductance is 8 μH and the leakage inductance is less than 0.5%. The constructed transformer is a prototype, so the core structure still needs some size optimization. For example, the length of the top and bottom bars is unnecessarily long as shown in Fig. 6. The final prototype will use the right size of the bars for the optimum size of the core.

5. Simulation Results:

Before the implementation step, comprehensive simulations are done to verify the design, also to determine some of the hardware requirements. For example, current ratings of the capacitors, inductors, cables, and so on can be easily determined from the simulation results. It is hard to determine RMS ratings by means of only analysis since the current through these elements include several components with different frequencies.

From the simulation results. It is hard to determine RMS ratings by means of only analysis since the current through these elements include several components with different frequencies.

6. References:

1. Solar energy (2013, July 23). [Online]. Available: http://www.conserve-energy-future.com/SolarEnergy.php
2. Europe Photovoltaic Industry Association (EPIA) (2013, July 23) Global market outlook for photovoltaics 2013–2017, [Online]. Available: http://www.epia.org/news/publications
3. Y. Xue, L. Chang, S. B. Kjaer, J. Bordonau, and T. Shimizu, "Topolo-gies of single-phase inverters for small distributed power generators: An overview," IEEE Trans. Power Electron., vol. 19, no. 5, pp. 1305–1314, Sep. 2004.
4. S. B. Kjaer, J. K. Pedersen, and F. Blaabjerg, "A review of single-phase grid-connected inverters for photovoltaic modules," IEEE Trans. Ind. Appl., vol. 41, no. 5, pp. 1292–1306, Sep. 2005.
5. Y. Li and R. Oruganti, "A low cost flyback CCM inverter for AC module application," IEEE Trans. Power Electron., vol. 27, no. 3, pp. 1295–1303, Mar. 2012.
6. N. Kasa, T. Iida, and L. Chen, "Flyback inverter controlled by sensorless current MPPT for photovoltaic power system," IEEE Trans. Ind. Electron., vol. 52, no. 4, pp. 1145–1152, Aug. 2005.
7. N. Mohan, T. M. Undeland, and W. P. Robbins, Power Electronics: Con-verters,

Applications, and Design. New York, NY, USA: Wiley, 2002.

8. C. Olalla, D. Clement, M. Rodriguez, and D. Maksimovic, "Architectures and control of submodule integrated DC–DC converters for photovoltaic applications," IEEE Trans. Ind. Appl., vol. 28, no. 6, pp. 2980–2997, Jun. 2013.
9. G. H. Tan, J. Z. Wang, and Y. C. Ji, "Soft-switching flyback inverter with enhanced power decoupling for photovoltaic applications," Electr. Power Appl., vol. 1, no. 2, pp. 264–274, Mar. 2007.
10. Z. Zhang, X.-F. He, and Y.-F. Liu, "An optimal control method for pho-tovoltaic grid-tied-interleaved flyback microinverters to achieve high ef-ficiency in wide load range," IEEE Trans. Ind. Appl., vol. 28, no. 11, pp. 5074–5087, Nov. 2013.
11. H. Hu, S. Harb, X. Fang, D. Zhang, Q. Zhang, Z. J. Shen, and I. Batarseh, "A three-port flyback for PV microinverter applications with power pul-sation decoupling capability," IEEE Trans. Power Electron., vol. 27, no. 9, pp. 3953–3964, Sep. 2012.
12. H. Hu, S. Harb, N. H. Kutkut, Z. J. Shen, and I. Batarseh, "A single-stage microinverter without using electrolytic capacitors," IEEE Trans. Power Electron., vol. 28, no. 6, pp. 2667–2687, Jun. 2013.
13. Y. M. Chen and C. Y. Liao, "Three-port flyback-type single-phase micro-inverter with active power decoupling circuit," in Proc. IEEE Energy Convers. Congr. Expo., 2011, pp. 501–506.
14. M. Gao, M. Chen, Q. Mo, Z. Qian, and Y. Luo, "Research on output current of interleaved-flyback in boundary conduction mode for photovoltaic AC module application," in Proc. IEEE Energy Convers. Congr. Expo., 2011, pp. 770–775.
15. C. Nanakos, E. C. Tatakis, and N. P. Papanikolaou, "A weighted-efficiency-oriented design methodology of flyback inverter for AC photo-voltaic modules," IEEE Trans. Power Electron., vol. 27, no. 7, pp. 3221– 3233, Jul. 2012.
16. Y.-H. Kim, Y.-H. Ji, J.-G. Kim, Y.-C. Jung, and C.-Y. Won, "A new control strategy for improving weighted efficiency in photovoltaic AC module-type interleaved flyback inverters," IEEE Trans. Power Electron., vol. 28, no. 6, pp. 2688–2699, Jun. 2013.
17. T. Shimizu, K. Wada, and N. Nakamura, "Flyback-type single-phase utility interactive inverter with power pulsation decoupling on the DC input for an AC photovoltaic module system," IEEE Trans. Power Electron., vol. 21, no. 5, pp. 1264–1272, Sep. 2006.
18. Y.-H. Kim, J.-G. Kim, Y.-H. Ji, C.-Y. Won, and T.-W. Lee, "Flyback inverter using voltage sensorless MPPT for AC module systems," in Proc. Int. Power Electron. Conf., 2010, pp. 948–953.
19. Z. Liang, R. Guo, J. Li, and A. Q. Huang, "A high-efficiency PV module integrated DC/DC converter for PV energy harvest in FREEDM systems," IEEE Trans. Power Electron., vol. 26, no. 3, pp. 897–909, Mar. 2011.
20. S. Zengin, F. Deveci, and M. Boztepe, "Decoupling capacitor selection in DCM flyback PV microinverters considering harmonic distortion," IEEE Trans. Power Electron., vol. 28, no. 2, pp. 816–825, Feb. 2013.